Minireveiw

Photoacoustic image-guided interventions

Madhumithra S Karthikesh[1] and Xinmai Yang[1,2]

[1]Bioengineering Program and Institute for Bioengineering Research, University of Kansas, Lawrence, KS 66045, USA; [2]Department of Mechanical Engineering, University of Kansas, Lawrence, KS 66045, USA
Corresponding author: Xinmai Yang. Email: xmyang@ku.edu

Impact statement

Photoacoustic imaging is an emerging modality for use in image-guided interventional procedures. This imaging technology has a unique ability to offer real-time, non-invasive, cost-effective, and radiation-free guidance in a real-world operating environment. This is substantiated in this article which sums up the current state and underlines promising results of research using photoacoustic imaging in guiding drug delivery, therapy, surgery, and biopsy. Hence, this minireview facilitates future research and real-world application of photoacoustic image-guided interventions.

Abstract

Photoacoustic imaging has demonstrated its potential for diagnosis over the last few decades. In recent years, its unique imaging capabilities, such as detecting structural, functional and molecular information in deep regions with optical contrast and ultrasound resolution, have opened up many opportunities for photoacoustic imaging to be used during image-guided interventions. Numerous studies have investigated the capability of photoacoustic imaging to guide various interventions such as drug delivery, therapies, surgeries, and biopsies. These studies have demonstrated that photoacoustic imaging can guide these interventions effectively and non-invasively in real-time. In this minireview, we will elucidate the potential of photoacoustic imaging in guiding active and passive drug deliveries, photothermal therapy, and other surgeries and therapies using endogenous and exogenous contrast agents including organic, inorganic, and hybrid nanoparticles, as well as needle-based biopsy procedures. The advantages of photoacoustic imaging in guided interventions will be discussed. It will, therefore, show that photoacoustic imaging has great potential in real-time interventions due to its advantages over current imaging modalities like computed tomography, magnetic resonance imaging, and ultrasound imaging.

Keywords: Photoacoustic imaging, image-guided intervention, drug delivery, surgery, noninvasive therapy, biopsy

***Experimental Biology and Medicine* 2020; 245: 330–341. DOI: 10.1177/1535370219889323**

Introduction

Photoacoustic imaging (PAI), also called as optoacoustic imaging, is an emerging clinical imaging modality that combines the merits of optical and ultrasound imaging (US).[1–5] In PAI, a target emits photoacoustic waves after being illuminated by short-duration laser pulses. The produced PA waves will then be detected by an ultrasound transducer for imaging.[1,4] The image contrast in PAI depends on the optical absorption and is independent of its mechanical properties and elasticity.[3] The spatial resolution of PAI is scalable with a penetration depth up to 5 cm, which is much deeper than pure optical imaging techniques in soft tissue.[1,3]

PAI has a lot of potentials in clinical diagnosis of various diseases, such as cancer, stroke, atherosclerosis, arthritis, etc. Applications of PAI in cancers include early detection, identifying the stages and metastasis, treatment planning and evaluation.[6–12] PAI is revealed to be successful in the diagnosis of breast,[13–19] prostate,[20–26] thyroid,[27–31] melanoma,[32–36] and ovarian[37–41] cancers. In stroke, PAI is utilized for imaging and understanding mechanical thrombolysis,[42] vessel segmentation,[43] and other vessel injuries that are caused by stroke in the brain.[44] In atherosclerosis, PAI helps in evaluating plaque distinction[45] and characterization,[46] and macrophage[47] and lipid[48] detection in the plaques. PAI has also been applied in arthritis for inflammation identification,[49,50] staging,[51] and evaluation.[52]

As an emerging modality, PAI can offer unique capabilities to visualize tissue structurally and functionally. The acquired structural and functional information can directly aid other diagnostic and therapeutic procedures. As a result, PAI has been widely used to guide other interventions such as drug delivery, therapies, biopsy, and surgeries. PAI is a promising modality for guiding interventions because of a wide range of advantages that it offers in real-time over current imaging techniques like

Copyright © 2019 by the Society for Experimental Biology and Medicine

the US, magnetic resonance imaging (MRI) and computed tomography (CT). Advantages of PAI-guided interventions in real-time are as follows: (1) non-invasiveness; (2) continuous imaging of structures during interventions; (3) sensitive, faster and inexpensive compared to MRI and CT; (4) only existing modality that can provide non-invasive penetration depth in the order of centimeters with optical contrast and ultrasound resolution; (5) acoustically dependent spatial resolution which is completely independent of optical absorption; (6) ability to function independently without requiring any external contrast agents and using intrinsic agents like hemoglobin and melanin; (7) safe as it does not produce any ionizing emission; (8) concurrent measurements of functional parameters like oxygen and hemoglobin level, temperatures, etc. by only using endogenous agents; (9) great optical contrast that highlights blood vessels; and (10) easily incorporated into the current operating environment with no laborious efforts.[1,3,53–72]

Because of the aforementioned advantages, PAI-guided intervention has enormous potential for enhancing the effectiveness of many treatments and therapies. Its application covers a broad range from cells to an entire organ system in the body.[73] PAI-guided interventions have been developed to use in cardiovascular system,[74,75] spinal system,[62] nerves,[65,76] tendons,[76] fetus,[77] lymph nodes,[14,78] and tumor occurring at different sites in the body.[66,67,78–82] It is extensively used for monitoring delivered drug,[83–87] and observing disease conditions, therapeutic outcomes, and subsequent tissue responses.

The overall structure of this minireview is summarized in Figure 1. This review is focused on exploring the advances in PAI-guided drug delivery, surgeries, therapies, and biopsies. PAI is capable of guiding precise drug release, monitoring drug distribution, and subsequent therapeutic effect. It can guide both passively and actively targeted deliveries. It also shows great potential in guiding surgeries mainly with the help of endogenous contrast agents to find the target and protect the surrounding structures. PAI is also a powerful tool for guiding photothermal therapy (PTT), chemo-PTT, chemo-photoacoustic and synergistic PTT and photoacoustic therapies by using various kinds of organic, inorganic, and hybrid nanoparticles. Further, it can also guide biopsies in real-time. Hence, this minireview intends to highlight the capability of PAI in guiding these interventions in real-time.

PAI-guided drug delivery

PAI is a promising imaging modality for guiding drug delivery because it can offer optical contrast with great penetration depth.[53] PAI can exploit the rich optical contrast of drug itself for contrast enhancement when there is a significant difference in optical absorption between tissue and the drug.[54] PAI also offers good sensitivity[55] and high spatial resolution.[56–59] Additionally, PAI is low cost in comparison MRI and CT, and can be used for real-time monitoring. Further, PAI can be easily incorporated with current clinical procedures, and easy to be operated by physicians.[60]

PAI has been used to track the route of drug administration,[88] and monitor drug release from its carrier, and the subsequent diffusion process and final distribution.[55,89–96] PAI has also been used to observe the therapeutic effects of drugs in real-time.[86] PAI-guided drug delivery is shown to be successful in cancer therapy,[89–93,95] anticoagulation therapy,[55,96] bipolar disease treatment,[94] and coronary heart disease treatment.[88] The investigation and validation of PAI for continuous monitoring are done on tissue/tumor phantoms,[93] animal models[92,95] and cell cultures[90,91] by

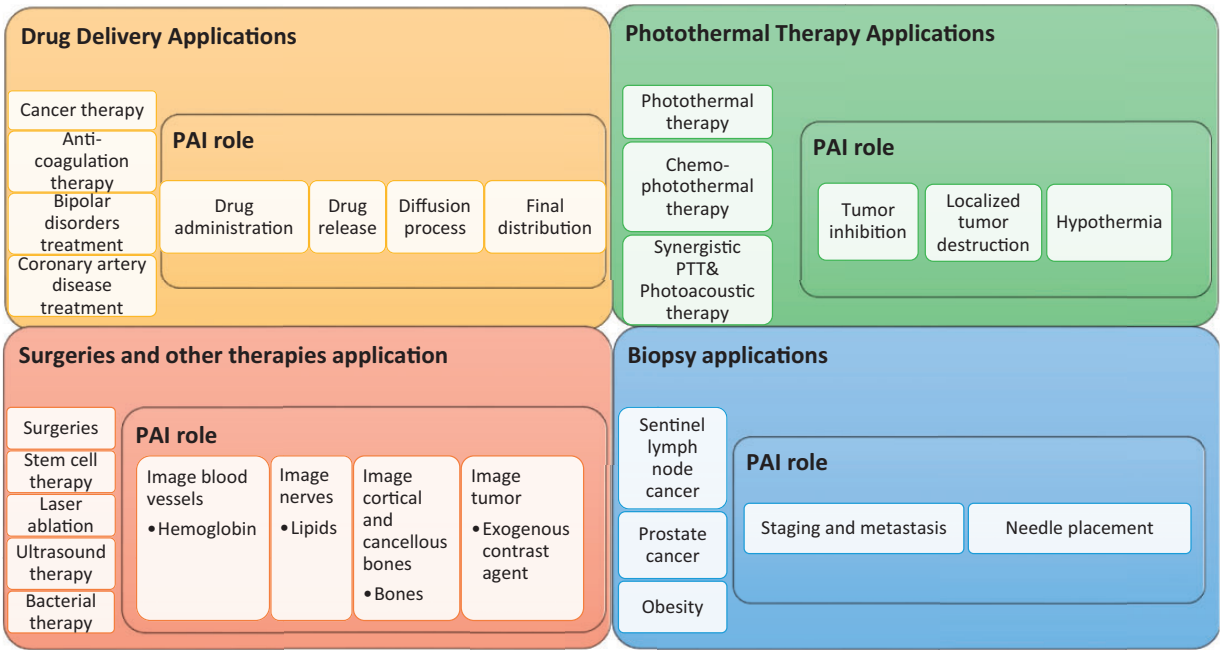

Figure 1. Overall structure of this review article with the applications discussed and PAI's role in each of the applications. (A color version of this figure is available in the online journal.)

either directly using the drug[88,90,91,95]/therapeutic agents[55,94,96] or using a dye that mimics the drug.[89,92,93]

Although sometimes free agents can be directly used,[93,96] nanoparticles are the most commonly used exogenous contrast agents for contrast enhancements in PAI-guided drug delivery. A vast number of inorganic nanomaterials such as metallic and carbon-based nanomaterials have been developed due to their desired optical properties for use as contrast and therapeutic agents. Recently, organic and semiconducting nanomaterials have also been deployed in photoacoustic theranostic applications.[87] Overall, drug delivery may be either passive or active targeting delivery. In passive drug delivery, the positive outcome of a drug depends on the amount of time it is present in circulation, whereas, in active drug delivery, the nanoparticles are tailor-made to bind specifically to a target.

PAI-guided passive drug delivery

PAI supports both passive and active targeting drug delivery, which are summarized in Table 1. PAI can guide passive delivery of drugs through enhanced permeability and retention effect as well as by coating nanoparticles with materials like polyethylene glycol (PEG).[97] Micelles loaded with doxorubicin (DOX) were used to investigate the PAI-guided passive drug delivery.[90] This was studied in the acidic lysosome environment of phantoms made using human breast cell lines. PAI successfully monitored the release of DOX and provided real-time visualization of micelles which were entering the lysosomes through endocytosis. PAI was investigated for passively monitoring heparin concentration using photoacoustic sensors.[96] These sensors were made up of cellulose and Neil blue A and were used for instantaneous monitoring of heparin concentration in plasma and blood. It was found that PAI could measure heparin concentration in the plasma and the blood in 3 min and 6 min, respectively.

PAI-guided active targeted delivery

PAI is extensively investigated for active targeted drug delivery using substances like nanoparticles or conjugated nanoparticles and free agents that can specifically bind to the target site. One study investigated PAI-guided controlled release of paclitaxel to folate expressing tumor cells using folate tagged nanorods containing paclitaxel, and the paclitaxel release was validated both *in vitro* using breast cancer cell line and *in vivo* in fibroblasts of mice.[91] Another study demonstrated that PAI-guided instantaneous monitoring of heparin levels is quick and non-invasive during anticoagulation therapy.[55] The methylene blue was capable of directly binding to the heparin present in the blood. This enabled PAI to monitor heparin levels in plastic tubes containing whole blood and methylene blue dye. PAI could measure the heparin levels in blood in 32 s. Figure 2(a) shows the PAI of plastic tubing of blood with varying heparin levels using methylene blue as a contrast agent for imaging.

In active drug delivery, the nanoparticles enable temperature, ultrasound pulse, and pH-controlled release of drugs

Table 1. Advances in applications of PAI-guided drug delivery.

Active/passive targeting	Application	Nanoparticles	Drugs /therapeutic agents /dye	Targets tested	PAI role	Ref.
Passive	Cancer therapy	PEG-modified poly (b-amino ester) graft copolymers, folic acid conjugated paclitaxel, perfluoro hexane and gold nanorods loaded nanoparticles	Doxorubicin, paclitaxel	Human breast cancer cells, human epithelial carcinoma cells and mouse embryonic fibroblast cells	Monitoring the drug release, drug release and synergistic chemo-photoacoustic therapy	90, 91
	Anticoagulation therapy	N/A	Heparin	Whole blood and plasma samples	Detects concentration of heparin	96
Active	Cancer therapy	Gold nanocages, doxorubicin, hydroxyl-based perylene diimide, and NIR dye 825 containing nanoparticles, perfluorocarbon-based nanoemulsion	Rhodamine 6G and methylene blue, Janus green B, doxorubicin, indocyanine green	Polyacrylamide phantom containing titanium oxide, U87MG glioma cell line and U87MG tumor model, vessel containing oxygenated canine blood	Monitoring the release of dyes through contrast enhancement, dye diffusion, pH-responsive drug release, drug release in treatments	89, 92, 93, 95
	Bipolar disorders treatment	Optode-based nanosensors	Lithium	Chicken muscle tissue	Physiological range of lithium	94
	Anticoagulation therapy	Agar gel and silica nanoparticles	Heparin	Plastic tubing containing whole blood	Detection of heparin concentration	55
	Coronary heart disease treatment	N/A	Drug-eluting stent	Porcine heart	Track cardiac drug delivery.	88

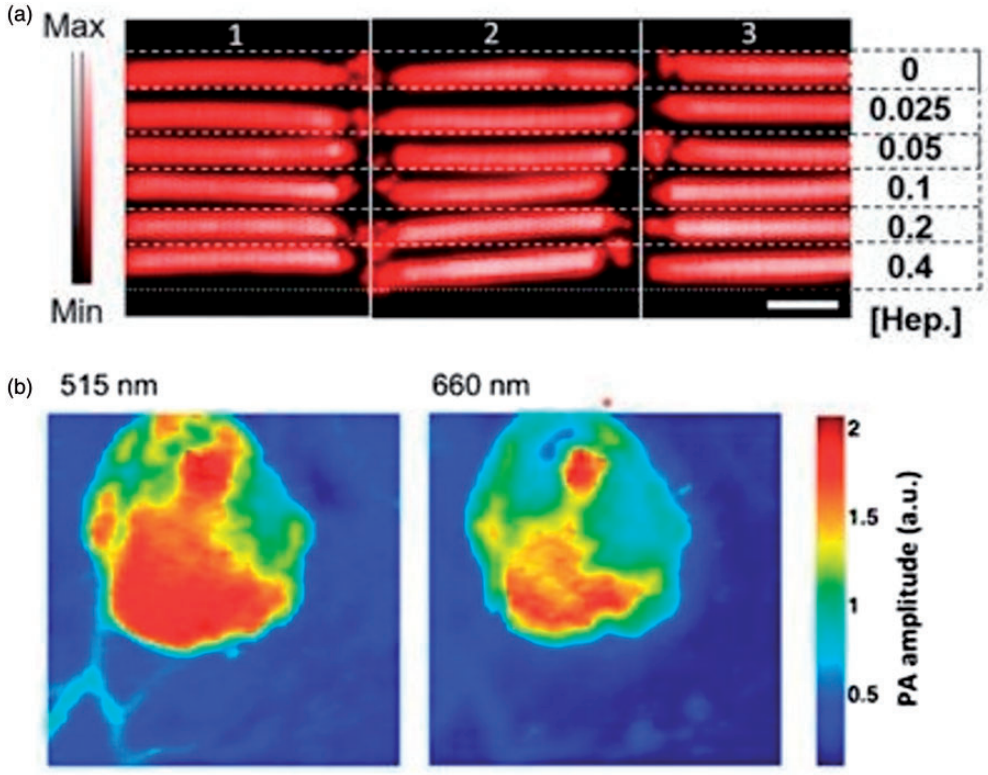

Figure 2. PAI-guided drug delivery. (a) PAI of three replicates of plastic tubing holding blood with increasing concentrations of heparin along with same concentration of methylene blue. Reprinted (adapted) with permission from Wang J, Chen F, Arconada-Alvarez SJ, Hartanto J, Yap LP, Park R, Wang F, Vorobyova I, Dagliyan G, Conti PS, Jokerst JV, A nanoscale tool for photoacoustic-based measurements of clotting time and therapeutic drug monitoring of heparin. *Nano Lett* 2016;**16**:6265–71. Copyright © 2016 American Chemical Society. (b) Photoacoustic tomography of injection boundary of lithium-based sensors into mice. Reprinted (adapted) with permission from Cash KJ, Li C, Xia J, Wang LV, and Clark HA, Optical Drug Monitoring: Photoacoustic Imaging of Nanosensors to Monitor Therapeutic Lithium in Vivo. *ACS Nano* 2015;**9**:1692–98. Copyright © 2015 American Chemical Society. (A color version of this figure is available in the online journal.)

in the target. Moon *et al.*[89] studied the temperature-controlled release of dyes Rhodamine 6G and methylene blue using high-intensity focused ultrasound (HIFU) and PAI. These dyes were chosen as they mimic cancer drugs. PAI contrast was enhanced by using gold nanocages containing HIFU pulse changing material. This study demonstrated the capability of PAI in guiding controlled drug release during cancer therapies like photothermal and chemotherapies. But the testing was not done using any real-world cancer drugs, and the concept was also not confirmed *in vivo.* PAI-guided pH-controlled release of DOX in the acidic environment was demonstrated.[95] In this study, theranostic perylene diimide responsive to pH was used. These platforms released DOX when they were in contact with weakly acidic tumor environment. PAI has demonstrated potential for concurrently imaging environmental pH and DOX release both *in vivo* in tumor containing live mice and *in vitro* using cancer cell lines. PAI was also capable of monitoring lithium levels with high quality and high penetration supporting the treatment of bipolar disorders (Figure 2(b)).[94] Photoacoustic nanosensors sensitive to lithium were used. These nanosensors experienced a pH change on encountering lithium in chicken muscle tissue. It resulted in changes in photoacoustic spectrum. This was exploited by PAI to monitor lithium level and continuously measure lithium concentration in the tissue using the nanosensors. This study proved that PAI had advantages over techniques like fluorescent and multiphoton imaging in monitoring lithium levels.

The drug may be conjugated with or encapsulated within the nanocarriers during the active drug delivery. This stimulates precise drug delivery into the target site. Indocyanine green (ICG), a dye that mimics the cancer drugs was incorporated into a perfluorocarbon-based emulsion to study the PAI-guided drug delivery.[92] It has been shown that PAI could improve ICG administration without altering the photoacoustic spectrum. Another study used *in situ* forming implants carrying dissolved Janus green B for monitoring the diffusion of dye.[93] It was tested on a tissue model made of polyacrylamide using PAI and quantitative US. The implants with dissolved dyes were injected as a liquid and then solidified inside the model. It was concluded in the study that PAI provided visualization of dye diffusion in real-time, while the US helped observe the changes in the state of these implants. Additionally, PAI showed great potential in addressing the problem of coronary restenosis due to coronary artery disease treatment. Though the development of drug eluted stent addressed this problem to a considerable extent, about 20% of those with these stents were still facing this problem.[88] To address this problem, the stent was coated with a drug surrogate, 1,1′-dioctadecyl-3,3,3′,3′-tetramethylindocarbocyanine perchlorate. PAI was successful in constantly monitoring the drug delivery

in the porcine heart. This proved the possibility of a reduced likelihood of occurrence of restenosis monitored by PAI.

PAI-guided photothermal therapy

The recent advancements in PAI-guided therapies have led to the development of numerous nanoparticle-based contrast agents. The nanoparticles used in PTT usually possess a higher absorbance in the near-infrared (NIR) region of the spectrum.[86] When irradiated with a laser, these nanoparticles results in ablation and death of the targeted cells confined to a small area.[98] As the heating effects due to absorption increase the body temperature above the normal 37°C, it results in hyperthermia. Depending on the amount of temperature increase, the effects may range from denaturation of proteins to permanent cell death.[99] PAI-guided PTT utilizes nanoparticles that may be an organic, inorganic or organic-inorganic hybrid.

PAI-guided PTT using organic nanoparticles

Organic nanoparticles are used as contrast agents in PAI-guided PTT as they possess excellent biocompatibility[73,100] and great drug packing capability.[73] The organic nanoparticles include polymers, conjugated polymers, and micelle-based nanoparticles. Polypyrrole is an organic polymer which possesses excellent conductivity, stability, and strong absorption in NIR range.[101] Chitosan which is an oceanic biological polymer possesses desirable characteristics like biocompatibility, cheap, plentiful, stable, and harmless. A combination of chitosan-polypyrrole nanoparticles is a preferred agent for confined tumor PTT as it holds preferred properties like biocompatibility and efficient PTT conversion. These were used in PAI-guided photothermal ablation of tumor in which the cells underwent apoptotic cell death after reaching tissue temperature of 62°C with the help of PAI to locate the tumor accurately. Conjugated polymeric nanoparticles caused cell necrosis in PAI-guided PTT.[102] These conjugated polymeric nanoparticles were decorated with amino acid ligand. These nanoparticles facilitated PAI in guiding the therapy by providing high contrast and signal-to-noise ratio. This allowed imaging of more profound structures. These nanoparticles also functioned as a great PTT agent for localized destruction of tumor. Melanin-based micelles are ideal as they are biocompatible, eco-friendly, and have high PTT efficiency.[103] PAI-guided PTT using melanin-based micelles with poly-L-lysine loaded with drug imitate on its surface was confirmed to increase the efficiency of the PTT. This increase in PTT efficiency was because PAI helped to refine NIR irradiation time on tissue and this caused cell necrosis in tumor.

PAI-guided PTT using inorganic nanoparticles

Inorganic nanoparticles for PAI-guided PTT include metallic nanoparticles, plasmonic nanoparticles, carbon-based nanoparticles, and quantum dots. The metallic nanoparticles like gold nanorods can be used as both PAI and PTT agent as they possess rich optical absorption and surface plasmon resonance (SPR).[8,104] But these have safety issues in the long run.[105] Silica-coated gold nanorods have greater thermal strength and intensify the photoacoustic signal to a great extent.[105] They were successfully used in PAI-guided PTT as they caused cell death in tumor tissue. The whole process was continuously monitored by PAI through temperature measurements. Combined PAI and US-guided PTT showed that these nanoparticles could produce preferred heat during therapies. Plasmonic nanoparticles are widely employed in PTT as their absorbance peaks are tunable by controlling their surface plasmon resonance during their synthesis.[106] Hence, by synthesizing these nanoparticles with a desired resonating wavelength in the NIR region, they can serve both as ideal contrast agents in PAI and photothermal agents in PTT. Gold nanoparticles are excellent examples of plasmonic nanoparticles in PAI-guided PTT. For example, gold nanorods offering both high PTT efficiency and NIR absorbance were loaded with graphene oxide, which offers excellent drug packing capacity.[106] These nanocrystals were successful in cancer therapy at tumor site of nude mice. Initially, PAI aided in drug release based on the change in the pH of the medium. This was then followed by PTT using the same gold nanorods. In the other study, gold nanostars conjugated with antibody of CD44v6, which is a surface marker that is expressed on gastric cancer cells,[107] was proven to be successful in destroying cancer cells through PTT using PAI for guidance. The same study demonstrated successful inhibition of tumor growth and increased lifetime of tumor-bearing mice using PTT, whereas PAI was used to calculate the PTT response of the cell. Superparamagnetic carbon-based nanoparticles are of significance as they can be used for multiple purposes, including when imaging using MRI and PAI as well as during therapies like PTT.[108] Hägg iron carbide is a superparamagnetic carbon-based nanoparticle that offers extraordinary absorption in NIR range and high PTT conversion efficiency. This can be used to treat the tumor without injuring the nearby tissue. These nanoparticles successfully aided tumor tissue to reach a temperature of about 47°C and to lead to necrotic and apoptotic cell death during PTT. The nanoparticles also enabled PAI to provide contrast enhancement and subsurface tissue organization in PAI-guided PTT. Copper chalcogenides are one of the quantum dots that can serve both as PTT and PAI agents due to their extraordinary NIR absorption and confined SPR.[109] They could be combined with iron oxide to produce tiny, biocompatible and versatile nanodots, and have also been applied in both MRI and NIR imaging.

PAI-guided PTT using hybrid nanoparticles

Hybrid nanomaterials containing both organic and inorganic nanomaterials are used as contrast agents in PAI-guided PTT captivating advantage of desirable properties of both. Hybrid PEGylated liposomes nanocarrier encapsulating melanin were designed.[110] These nanocarriers showed excellent biocompatibility. They destroyed tumor completely and increased the PTT conversion efficiency during therapy. PAI was used to guide PTT by enabling the monitoring of their distribution.

Composite tantalum oxide nanoparticles contained in polypyrrole nanoparticles served as both good photothermal and PAI contrast agents.[111] They showed great compatibility as well as PTT conversion efficiency with high absorption in the NIR region. These nanoparticles showed great promise in PAI-guided PTT both *in vivo* and *in vitro*.

PAI-guided PTT combined with other therapies

PAI can also guide PTT combined and other therapies including chemo-photothermal therapy,[112,113] chemo-photoacoustic therapy,[91] and synergistic PTT and photoacoustic therapy.[81] The nanoparticles used in chemotherapy result in hypothermic heating effect when irradiated with laser. This heating is used to increase the diffusion rate of nanoparticles, thereby increasing their uptake by cells as a result of an increase in cellular permeability.[114,115] PAI-guided chemo-photothermal therapy using conjugated polymeric nanoparticles caused cell death in tumor.[112] Polydopamine nanoparticles are of huge interest recently since they structurally resemble melanin. They have excellent biocompatibility and high optical absorption in the NIR range. They also have potential to stack drugs in them. Being inexpensive, polydopamine nanoparticle along with peptide was found to be a promising agent for contrast enhancement in PAI. Additionally, they were also therapeutic agents for chemo-photothermal therapy. They helped to reach 52°C in tumor tissue. This caused cell death, which can be monitored by high contrast-enhanced PAI.[112] Another study showed that PAI-guided chemo-PTT using hybrid mesoporous silica loaded with Prussian blue was successful.[113] This hybrid nanoparticle combined the benefits of mesoporous silica and Prussian blue. Mesoporous silica is stimuli-responsive and can precisely carry and release the drug. The Food and Drug Administration-(FDA) approved Prussian blue can serve as both PTT thermal agent and PAI contrast agent. These hybrid nanoparticles were used in PAI-guided chemo-photothermal therapy causing localized cell death in tumor tissue. They also functioned as an exogenous contrast agent for PAI allowing visualization of contrast-enhanced tumor morphology and molecular distribution. PAI successfully guided chemo-photoacoustic therapy using hybrid organo-inorganic conjugated nanoparticles containing paclitaxel, perfluorohexane, and gold nanorods.[91] They provided contrast enhancement for PAI and enabled quick drug release due to the evaporation of perfluorohexane. PAI-guided synergistic interaction of PTT and photoacoustic therapy on tumor using micelle-based nanoparticles was found to be capable of exactly locating and entirely destroying a solid tumor.[81] During PTT, the temperature of the cells increased to 45°C causing apoptotic cell death, which can be monitored by PAI in real-time with enhanced contrast. Figure 3 shows the PA images obtained from tumors in nude mice at 0, 6, 12, and 24-h post injection of these nanoparticles.

PAI-guided surgeries and other therapies

Other than PTT, PAI can non-invasively guide other surgeries and therapies that are minimally invasive or invasive in real-time. PAI can aid in the surgical intervention and therapy of tumor,[66,67,79,116] peripheral neuropathy,[76,117] pain,[65] fetal disorders,[77] and gastrointestinal diseases.[118] PAI plays different roles in different surgeries, including visualization[65,67,77,117,119] and differentiation[76,116] of structures. PAI can differentiate the cancellous and cortical bones,[116] tumor and normal tissue,[120] and nerves and tendons.[76] It ensures safety by enabling the visualization of nerves and vasculature, thereby avoiding any unexpected damage to these structures during surgeries. PAI can guide therapies by imaging deeper tissue,[82] temperature,[121] tumor,[113] and molecular distribution[113] along with contrast enhancement.

PAI-guided minimally invasive surgeries and other therapies

PAI enabled visualization of blood vessels[66,67,77] during surgeries and temperature[70] monitoring during therapies using the endogenous contrast agent hemoglobin for contrast enhancement. Image guidance is critical in guiding fetal surgeries such as anastomoses photocoagulation. Fetoscopy is currently used for guiding these surgeries. However, a large amount of light is scattered by soft tissue, which is not sensitive enough to image the vasculature below the placental surface. This will lead to partial photocoagulation and result in post-surgical problems and increased prenatal mortality. One study showed that PAI and US could be used simultaneously to image veins that lay beneath placenta obtained from a cesarean section.[77] It was found that PAI allowed visualization of the veins while US provided spatial position. During the removal of pituitary tumors, the carotid artery is hidden behind the sphenoid bone and causes injuries to it which may even lead to patient death. Though CT and MRI can support direction finding, finding arteries are indeterminate. With anticipated errors, PAI facilitated the visualization of the sphenoid bone and the blood vessels in a model comprising of the temporal bone and soft tissue.[67] PAI-guided telerobotic surgery was capable of localizing artery from the drill bit using da Vinci system without any damage to them.[66] PAI is also used for measuring the temperature during cryotherapy of prostate cancer in real time.[70] PAI along with US allowed continuous monitoring of temperature in canine prostate. As the photoacoustic response of blood varied with temperature, it provided temperature mapping non-invasively along with contrast enhancement.

PAI can also guide ultrasound therapy,[82] laser ablation,[121] targeted anti-bacterial therapy, and stem cell therapy. PAI provided deeper tissue imaging with enhanced contrast using gold nanorods during ultrasound therapy.[82] This study used an integrated system consisting of PAI and HIFU. The integrated system exhibited efficacy in focusing and treating the solid tumor by using gold nanorods as contrast agents. PAI can also guide laser ablation by using an organo-inorganic hybrid PEG conjugated gold nanorods holding DOX.[121] These hybrid nanorods are harmless and

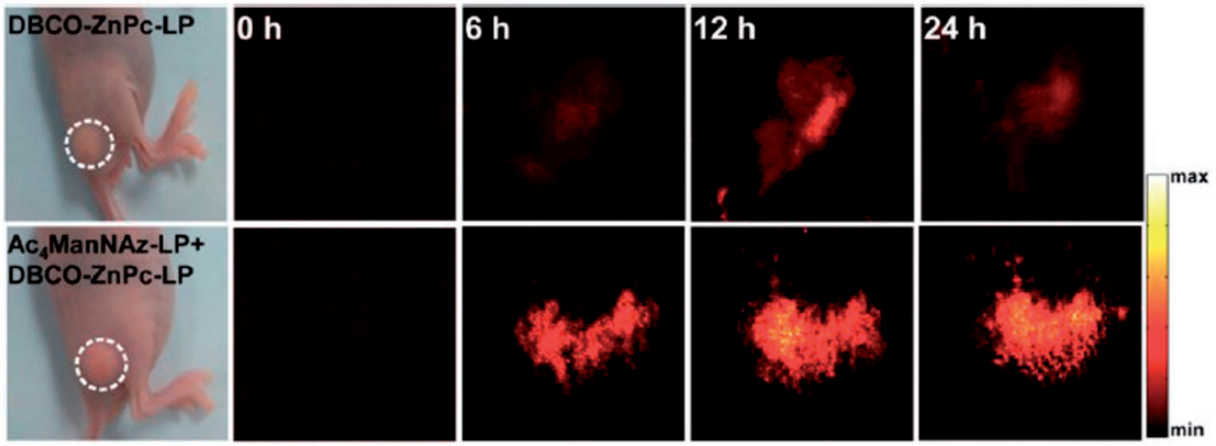

Figure 3. PAI obtained from tumor in nude mice at 0, 6, 12, and 24-h post-injection of the micelle-based nanoparticles. Reprinted (adapted) with permission from Du L, Qin H, Ma T, Zhang T, and Xing D, *In vivo* imaging-guided photothermal/photoacoustic synergistic therapy with biorthogonal metabolic glycoengineering-activated tumor targeting nanoparticles. *ACS Nano* 2017;11(9):8930–43. Copyright © 2017 American Chemical Society. (A color version of this figure is available in the online journal.)

resistant to immune response. They can selectively destroy the tumor cells with negligible injury to the surrounding cells. They caused cell necrosis at temperatures greater than 50°C. PAI monitored the temperature by using them as exogenous contrast agents. Silver ions have been used in targeted anti-bacterial therapies under PAI guidance.[122] Their release and bactericidal action were studied successfully on both Gram positive and Gram-negative bacteria. Silver is first coated on the gold nanorods resulting in reduced photoacoustic signal. But when this silver starts to get dissolved as silver ions in the infected tissues, the photoacoustic signal started increasing. This PAI-guided therapy of bacteria resulted in a low number of bacteria *in vivo* in mice. In cardiovascular stem cell therapies, trimodal contrast agent was designed for tracing the stem cells in the heart.[123] The contrast agent was selectively designed such that it contained iron oxide nanobubble, poly (lacto-co-gycolic acid) coating and 1,1′-dioctadecyl-3,3,3′,3′-tetramethylindotricarbocyanine iodide (DiR) for increasing the signal acquired during magnetic particle imaging, US, and PAI, respectively. The stem cells were successfully monitored and traced in live mice in real time using all the three imaging modalities. PAI was also demonstrated to be capable of tracking stem cell viability in real time.[124] This study employed gold nanorods coated with reactive oxygen species as a contrast agent for PAI. These nanorods were injected into the mesenchymal stem cells before transplantation into mice. Combined PAI-US successfully tracked the viability of stem cells in mice with excellent spatial and temporal resolution. Figure 4 shows ratiometric PAI of viable transplanted stem cells in mice acquired at 795 nm and 920 nm on various days of stem cell therapy.

PAI-guided invasive surgeries

PAI can guide peripheral nerve surgeries and prostatectomy using lipid as an endogenous contrast agent[76,117,119] for visualizing nerves. Peripheral nerve surgeries are performed for treating the peripheral blocks. These surgeries are common as many people are affected by it globally. It is critical to visualize the nerves during these surgeries to avoid any nerve injuries. However, diagnosis and treatment of these surgeries are limited as no modality could measure these fibers non-invasively. PAI was successfully employed in differentiating nerves from tendons with higher contrast.[76] This showed greater potential to avoid nerve punctures compared to US during the peripheral nerve surgery. PAI also enabled visualization of particular nerves with a better resolution by using lipid in myelin sheath as a contrast agent.[117] This was validated in chicken tissue. PAI along with transrectal ultrasound (TRUS) was confirmed to image periprostatic vessels and produce enhanced imaging of neurovascular bundle.[119] This was further validated with improved localization of a neurovascular bundle in seven cancer patients who underwent prostatectomy. This study showed that PAI and TRUS probe were better at visualizing neurovascular bundle than TRUS alone.

PAI can guide spinal fusion surgeries using bone as a contrast agent. Spine fusion surgeries are often designed to be precise to avoid any damage to the surrounding structures as it can lead to serious complications. PAI could non-invasively differentiate the cancellous and cortical bones. This was accomplished by using the difference in characteristics like amplitude and signal-to-noise ratio in the signals obtained from the different bones.[116]

PAI-guided tumor resection surgeries enhanced tumor visualization using iron oxide nanoparticles as external agents.[79,120] Patients undergoing tumor resection have increased survival on proper removal with no residues left. This greatly reduces the need for revision surgeries which would be cost-forbidden. These surgeries when guided by PAI showed a decreased local reappearance of tumor in a murine model with invasive mammary carcinoma.[79] The tumor was completely removed with superior contrast using targeted iron oxide nanoparticles. It was validated that no residue was left behind using fluorescence NIR. PAI guidance was also effective in preventing the

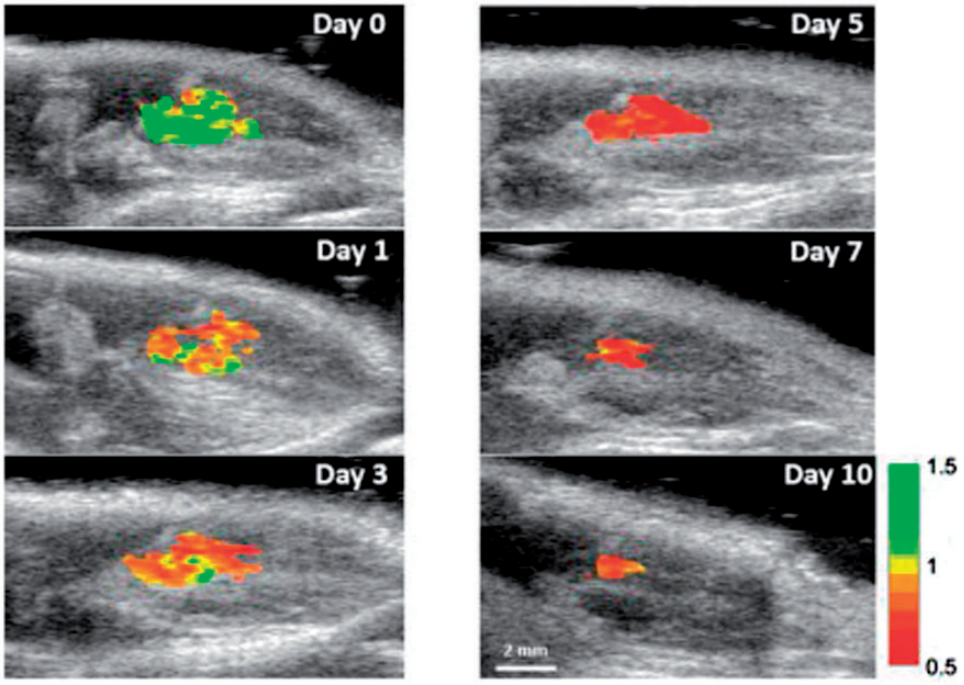

Figure 4. Ratiometric PAI of viable transplanted stem cells in mice acquired at 795 nm and 920 nm on 0, 1, 3, 5, 7, and 10th day of stem cell therapy. Reprinted (adapted) with permission from Dhada KS, Hernandez DS, and Suggs LJ, In vivo photoacoustic tracking of mesenchymal stem cell viability. *ACS Nano* 2019;**13**:7791–7799. Copyright © 2019 American Chemical Society. (A color version of this figure is available in the online journal.)

recurrence of the tumor due to partial resection in brain tumor surgery.[120] This showed an increase in the number of recurrence-free survivals in mice. MRI and PAI were used to locate tumor before and during surgery, respectively. This method used ICG and superparamagnetic iron oxide as contrast agents as both of these contrast agents were approved by the FDA.

PAI-guided biopsies

PAI is a promising tool for guiding biopsies as it is non-invasive and possesses a high penetration depth. PAI can play a crucial role in biopsies through real-time vision-based robot control of biopsy needle tips passage in obese patients,[125] and in staging cancer and detecting the metastasis during needle biopsy of sentinel lymph nodes[78] and prostate.[80] Needle biopsy remains puzzling in obese patients as the needle has to travel through many layers of fat and additional tissue leading to several needle passages. PAI-guided liver biopsies in these patients were revealed to be successful robotically with a negligible error rate using a transducer system placed in the middle of the needle.[125] PAI was used to guide sentinel lymph node biopsy using ICG as a contrast agent. The needle insertion was monitored continuously using PAI, demonstrating the capability of PAI.[78] Similar capability of PAI was also demonstrated in visualizing the tumor in canine prostate.[80]

Conclusions and future scope

Though PAI possesses significant advantages, it is also true that it holds some limitations on clinical translation. The first limitation is the use of exogenous contrast agents. As PAI frequently requires use of exogenous contrast agents, it brings in many safety concerns. The effects of the dyes over a long-term and their elimination from the body are the major issues as these agents could cause many deleterious effects in the body. Image artifacts reduction remains another notable problem during reconstruction of the photoacoustic image from the signals. This requires highly complicated algorithms and has a lengthy processing time. Imaging depth of PAI is also a notable limitation as the transport of light in soft tissue is strongly limited by the scattering of soft tissue.

PAI has a broader scope for translation with a range of new applications such as light emitting diode-based PAI (LED-based PAI), and wearable PAI. LED-based photoacoustic scanners are shown to be capable of measuring the reactive oxygen and nitrogen species.[126] This has been validated *in vivo* in mice. Wearable optical resolution photoacoustic microscopy (W-ORPAM) is one of the wearable PAI system used for imaging the cerebral cortex in real time.[127] This technology exploits the variation in vasculature under different physiological conditions and was tested in mice. Another wearable device using PAI for monitoring the periodontal health was proved to be successful and this was confirmed in human.[128]

In conclusion, though many imaging modalities are available for guiding interventions in real-time, PAI stands uniquely among them as it is non-invasive, safe, real-time, strong optical contrast, and sometimes does not even need any external contrast agents. Like other imaging modalities, PAI also has some limitations including imaging depth. But, as it is inexpensive, easy to operate, and has

strong imaging contrast, PAI-guided intervention holds great potential for fast clinical translation and may be preferred over other modalities under certain settings. PAI has been engaged in newer applications and has also been constantly evolving in its existing applications and could become commonly applied imaging modality for guiding interventions in real-time soon.

Authors' contributions: All the authors have contributed equally in writing and editing this article.

DECLARATION OF CONFLICTING INTERESTS

The author(s) declared no potential conflicts of interest with respect to the research, authorship, and/or publication of this article.

FUNDING

This work was supported in part through a National Institutes of Health (NIH) grant R01EY029489.

ORCID iD

Madhumithra S Karthikesh https://orcid.org/0000-0001-6397-9357

REFERENCES

1. Xu M, Wang LV. Photoacoustic imaging in biomedicine. *Rev Sci Instrum* 2006;**77**:041101
2. Sun Y, Jiang H, E. O'Neill B. Photoacoustic imaging: an emerging optical modality in diagnostic and theranostic medicine. *J Biosens Bioelectron* 2011;**2**:1000108
3. Beard P. Biomedical photoacoustic imaging. *Interf Focus* 2011;**1**:602–31
4. Wang LV. Tutorial on photoacoustic microscopy and computed tomography. *IEEE J Select Topics Quantum Electron* 2008;**14**:171–9
5. Choi W, Park E-Y, Jeon S, Kim C. Clinical photoacoustic imaging platforms. *Biomed Eng Lett* 2018;**8**:139–55
6. Valluru KS, Willmann JK. Clinical photoacoustic imaging of cancer. *Ultrasonography* 2016;**35**:267–80
7. Mehrmohammadi M, Yoon SJ, Yeager D, Emelianov SY. Photoacoustic imaging for cancer detection and staging. *Curr Mol Imaging* 2013;**2**:89–105
8. Mallidi S, Luke GP, Emelianov S. Photoacoustic imaging in cancer detection, diagnosis, and treatment guidance. *Trends Biotechnol* 2011;**29**:213–21
9. Chen Y-S, Yeager D, Emelianov SY. Chapter 9 – photoacoustic imaging for cancer diagnosis and therapy guidance. In: Chen X and Wong S (eds) *Cancer theranostics*. Oxford: Academic Press, 2014, pp. 139–58
10. Valluru KS, Wilson KE, Willmann JK. Photoacoustic imaging in oncology: translational preclinical and early clinical experience. *Radiology* 2016;**280**:332–49
11. Gargiulo S, Albanese S, Mancini M. State-of-the-art preclinical photoacoustic imaging in oncology: recent advances in cancer theranostics. *Contrast Media Mol Imaging* 2019;**2019**:24
12. Yang J, Zhang G, Li Q, Liao C, Huang L, Ke T, Jiang H, Han D. Photoacoustic imaging for the evaluation of early tumor response to antivascular treatment. *Quant Imaging Med Surg* 2019;**9**:160–70
13. Toi M, Asao Y, Matsumoto Y, Sekiguchi H, Yoshikawa A, Takada M, Kataoka M, Endo T, Kawaguchi-Sakita N, Kawashima M, Fakhrejahani E, Kanao S, Yamaga I, Nakayama Y, Tokiwa M, Torii M, Yagi T, Sakurai T, Togashi K, Shiina T. Visualization of tumor-related blood vessels in human breast by photoacoustic imaging system with a hemispherical detector array. *Sci Rep* 2017;**7**:41970
14. Garcia-Uribe A, Erpelding TN, Krumholz A, Ke H, Maslov K, Appleton C, Margenthaler JA, Wang LV. Dual-Modality photoacoustic and ultrasound imaging system for noninvasive sentinel lymph node detection in patients with breast cancer. *Sci Rep* 2015;**5**:15748
15. Neuschler EI, Butler R, Young CA, Barke LD, Bertrand ML, Bohm-Velez M, Destounis S, Donlan P, Grobmyer SR, Katzen J, Kist KA, Lavin PT, Makariou EV, Parris TM, Schilling KJ, Tucker FL, Dogan BE. A pivotal study of optoacoustic imaging to diagnose benign and malignant breast masses: a new evaluation tool for radiologists. *Radiology* 2018;**287**:398–412
16. Manohar S, Kharine A, van Hespen JC, Steenbergen W, van Leeuwen TG. The twente photoacoustic mammoscope: system overview and performance. *Phys Med Biol* 2005;**50**:2543–57
17. Zhang J, Chen B, Zhou M, Lan H, Gao F. Photoacoustic image classification and segmentation of breast cancer: a feasibility study. *IEEE Access* 2019;**7**:5457–66
18. Diot G, Metz S, Noske A, Liapis E, Schroeder B, Ovsepian SV, Meier R, Rummeny E, Ntziachristos V. Multispectral optoacoustic tomography (MSOT) of human breast cancer. *Clin Cancer Res* 2017;**23**:6912–22
19. Pramanik M, Ku G, Li C, Wang LV. Design and evaluation of a novel breast cancer detection system combining both thermoacoustic (TA) and photoacoustic (PA) tomography. *Med Phys* 2008;**35**:2218–23
20. Liu C, Xing M, Cong B, Qiu C, He D, Wang C, Xiao Y, Yin T, Shao M, Qiu W, Ma T, Gong X, Chen X, Zheng H, Zheng R, Song L. In vivo transrectal imaging of canine prostate with a sensitive and compact handheld transrectal array photoacoustic probe for early diagnosis of prostate cancer. *Biomed Opt Exp* 2019;**10**:1707–17
21. Ai M, Youn J-I, Salcudean SE, Rohling R, Abolmaesumi P, Tang S. Photoacoustic tomography for imaging the prostate: a transurethral illumination probe design and application. *Biomed Opt Exp* 2019;**10**:2588–605
22. Wang X, Roberts WW, Carson PL, Wood DP, Fowlkes JB. Photoacoustic tomography: a potential new tool for prostate cancer. *Biomed Opt Exp* 2010;**1**:1117–26
23. Su JL, Bouchard RR, Karpiouk AB, Hazle JD, Emelianov SY. Photoacoustic imaging of prostate brachytherapy seeds. *Biomed Opt Exp* 2011;**2**:2243–54
24. Patterson MP, Riley CB, Kolios MC, Whelan WM. Optoacoustic characterization of prostate cancer in an in vivo transgenic murine model. *J Biomed Opt* 2014;**19**:056008
25. Horiguchi A, Shinchi M, Nakamura A, Wada T, Ito K, Asano T, Shinmoto H, Tsuda H, Ishihara M. Pilot study of prostate cancer angiogenesis imaging using a photoacoustic imaging system. *Urology* 2017;**108**:212–9
26. Xu G, Qin M, Mukundan A, Siddiqui J, Takada M, Vilar-Saavedra P, Tomlins SA, Kopelman R, Wang X. Prostate cancer characterization by optical contrast enhanced photoacoustics. *Proc SPIE Int Soc Opt Eng* 2016;**9708**:97080I
27. Levi J, Kothapalli SR, Bohndiek S, Yoon JK, Dragulescu-Andrasi A, Nielsen C, Tisma A, Bodapati S, Gowrishankar G, Yan X, Chan C, Starcevic D, Gambhir SS. Molecular photoacoustic imaging of follicular thyroid carcinoma. *Clin Cancer Res* 2013;**19**:1494–502
28. Dogra VS, Chinni BK, Valluru KS, Moalem J, Giampoli EJ, Evans K, Rao NA. Preliminary results of ex vivo multispectral photoacoustic imaging in the management of thyroid cancer. *AJR Am J Roentgenol* 2014;**202**:W552–8
29. Gorey A, Jacob PM, Abraham DT, John R, Manipadam MT, Ansari MS, Chen GCK, Vasudevan S. Differentiation of malignant from benign thyroid nodules using photoacoustic spectral response: a preclinical study. *Biomed Phys Eng Exp* 2019;**5**:035017
30. Yang M, Zhao L, He X, Su N, Zhao C, Tang H, Hong T, Li W, Yang F, Lin L, Zhang B, Zhang R, Jiang Y, Li C. Photoacoustic/ultrasound dual imaging of human thyroid cancers: an initial clinical study. *Biomed Opt Exp* 2017;**8**:3449–57
31. Kim J, Kim M-H, Jo K, Ha J, Kim Y, Lim D-J, Kim C. Photoacoustic analysis of thyroid cancer in vivo: a pilot study. *SPIE* 2017;**10064**:1006408

32. Weight RM, Viator JA, Dale PS, Caldwell CW, Lisle AE. Photoacoustic detection of metastatic melanoma cells in the human circulatory system. *Opt Lett* 2006;**31**:2998–3000
33. Galanzha EI, Shashkov EV, Spring PM, Suen JY, Zharov VP. In vivo, noninvasive, label-free detection and eradication of circulating metastatic melanoma cells using two-color photoacoustic flow cytometry with a diode laser. *Cancer Res* 2009;**69**:7926–34
34. Wang Y, Maslov K, Zhang Y, Hu S, Yang L, Xia Y, Liu J, Wang LV. Fiber-laser-based photoacoustic microscopy and melanoma cell detection. *J Biomed Opt* 2011;**16**:011014
35. Khattak S, Gupta N, Zhou X, Pires L, Wilson BC, Yucel YH. Non-invasive dynamic assessment of conjunctival melanomas by photoacoustic imaging. *Exp Eye Res* 2019;**179**:157–67
36. Zhou Y, Li G, Zhu L, Li C, Cornelius LA, Wang LV. Handheld photoacoustic probe to detect both melanoma depth and volume at high speed in vivo. *J Biophoton* 2015;**8**:961–7
37. Salehi HS, Li H, Merkulov A, Kumavor PD, Vavadi H, Sanders M, Kueck A, Brewer MA, Zhu Q. Coregistered photoacoustic and ultrasound imaging and classification of ovarian cancer: ex vivo and in vivo studies. *J Biomed Opt* 2016;**21**:046006
38. Amidi E, Mostafa A, Nandy S, Yang G, Middleton W, Siegel C, Zhu Q. Classification of human ovarian cancer using functional, spectral, and imaging features obtained from in vivo photoacoustic imaging. *Biomed Opt Exp* 2019;**10**:2303–17
39. Bohndiek SE, Sasportas LS, Machtaler S, Jokerst JV, Hori S, Gambhir SS. Photoacoustic tomography detects early vessel regression and normalization during ovarian tumor response to the antiangiogenic therapy trebananib. *J Nucl Med* 2015;**56**:1942–7
40. Aguirre A, Ardeshirpour Y, Sanders MM, Brewer M, Zhu Q. Potential role of coregistered photoacoustic and ultrasound imaging in ovarian cancer detection and characterization. *Transl Oncol* 2011;**4**:29–37
41. Yang Y, Li X, Wang T, Kumavor PD, Aguirre A, Shung KK, Zhou Q, Sanders M, Brewer M, Zhu Q. Integrated optical coherence tomography, ultrasound and photoacoustic imaging for ovarian tissue characterization. *Biomed Opt Exp* 2011;**2**:2551–61
42. Berlis A, Lutsep H, Barnwell S, Norbash A, Wechsler L, Jungreis CA, Woolfenden A, Redekop G, Hartmann M, Schumacher M. Mechanical thrombolysis in acute ischemic stroke with endovascular photoacoustic recanalization. *Stroke* 2004;**35**:1112–6
43. Soetikno B, Hu S, Gonzales E, Zhong Q, Maslov K, Lee J-M, Wang LV. Vessel segmentation analysis of ischemic stroke images acquired with photoacoustic microscopy. *SPIE* 2012;**8223**:822345
44. Hu S, Gonzales E, Soetikno B, Gong E, Yan P, Maslov K, Lee J-M, Wang LV. Optical-resolution photoacoustic microscopy of ischemic stroke. *SPIE* 2011;**7899**:789906
45. Sethuraman S, Amirian JH, Litovsky SH, Smalling RW, Emelianov SY. Spectroscopic intravascular photoacoustic imaging to differentiate atherosclerotic plaques. *Opt Exp* 2008;**16**:3362–7
46. Sethuraman S, Amirian JH, Litovsky SH, Smalling RW, Emelianov SY. Ex vivo characterization of atherosclerosis using intravascular photoacoustic imaging. *Opt Exp* 2007;**15**:16657–66
47. Wang B, Yantsen E, Larson T, Karpiouk AB, Sethuraman S, Su JL, Sokolov K, Emelianov SY. Plasmonic intravascular photoacoustic imaging for detection of macrophages in atherosclerotic plaques. *Nano Lett* 2009;**9**:2212–7
48. Wang B, Su JL, Amirian J, Litovsky SH, Smalling R, Emelianov S. Detection of lipid in atherosclerotic vessels using ultrasound-guided spectroscopic intravascular photoacoustic imaging. *Opt Exp* 2010;**18**:4889–97
49. Wang X, Chamberland DL, Jamadar DA. Noninvasive photoacoustic tomography of human peripheral joints toward diagnosis of inflammatory arthritis. *Opt Lett* 2007;**32**:3002–4
50. Rajian JR, Girish G, Wang X. Photoacoustic tomography to identify inflammatory arthritis. *J Biomed Opt* 2012;**17**:96013
51. Beziere N, von Schacky C, Kosanke Y, Kimm M, Nunes A, Licha K, Aichler M, Walch A, Rummeny EJ, Ntziachristos V, Meier R. Optoacoustic imaging and staging of inflammation in a murine model of arthritis. *Arthritis Rheumatol* 2014;**66**:2071–8
52. Jo J, Xu G, Marquardt A, Girish G, Wang X. Photoacoustic evaluation of human inflammatory arthritis in human joints. *SPIE* 2017;**10064**:1006409
53. Ke H, Erpelding TN, Jankovic L, Liu C, Wang LV. Performance characterization of an integrated ultrasound, photoacoustic, and thermoacoustic imaging system. *J Biomed Opt* 2012;**17**:056010
54. Tang S, Chen J, Samant P, Stratton K, Xiang L. Transurethral photoacoustic endoscopy for prostate cancer: a simulation study. *IEEE Trans Med Imaging* 2016;**35**:1780–7
55. Wang J, Chen F, Arconada-Alvarez SJ, Hartanto J, Yap LP, Park R, Wang F, Vorobyova I, Dagliyan G, Conti PS, Jokerst JV. A nanoscale tool for Photoacoustic-Based measurements of clotting time and therapeutic drug monitoring of heparin. *Nano Lett* 2016;**16**:6265–71
56. Weber J, Beard PC, Bohndiek SE. Contrast agents for molecular photoacoustic imaging. *Nat Methods* 2016;**13**:639
57. Ku G, Wang LV. Deeply penetrating photoacoustic tomography in biological tissues enhanced with an optical contrast agent. *Opt Lett* 2005;**30**:507–9
58. Kim C, Favazza C, Wang LV. In vivo photoacoustic tomography of chemicals: high-resolution functional and molecular optical imaging at new depths. *Chem Rev* 2010;**110**:2756–82
59. Ntziachristos V. Going deeper than microscopy: the optical imaging frontier in biology. *Nat Methods* 2010;**7**:603
60. Donnelly EM, Kubelick KP, Dumani DS, Emelianov SY. Photoacoustic Image-Guided delivery of Plasmonic-Nanoparticle-Labeled mesenchymal stem cells to the spinal cord. *Nano Lett* 2018;**18**:6625–32
61. Eddins B, Bell MA. Design of a multifiber light delivery system for photoacoustic-guided surgery. *J Biomed Opt* 2017;**22**:41011
62. Han SH. Review of photoacoustic imaging for Imaging-Guided spinal surgery. *Neurospine* 2018;**15**:306–22
63. Kitazawa K, Okudera H, Takemae T, Kobayashi S. CT guided transsphenoidal surgery: report of nine cases. *No Shinkei Geka* 1993;**21**:147–52
64. Schwartz TH, Stieg PE, Anand VK. Endoscopic transsphenoidal pituitary surgery with intraoperative magnetic resonance imaging. *Neurosurgery* 2006;**58**:ONS44-51; discussion ONS44-51.
65. Xia W, Nikitichev DI, Mari JM, West SJ, Pratt R, David AL, Ourselin S, Beard PC, Desjardins AE. Performance characteristics of an interventional multispectral photoacoustic imaging system for guiding minimally invasive procedures. *J Biomed Opt* 2015;**20**:86005
66. Kim S, Tan Y, Kazanzides P, Bell MAL. Feasibility of photoacoustic image guidance for telerobotic endonasal transsphenoidal surgery. In: *6th IEEE international conference on biomedical robotics and biomechatronics (BioRob)*, Singapore, 26-29 Jun 2016.
67. Lediju Bell MA, Ostrowski AK, Li K, Kazanzides P, Boctor EM. Localization of transcranial targets for Photoacoustic-Guided endonasal surgeries. *Photoacoustics* 2015;**3**:78–87
68. Wang LV. Multiscale photoacoustic microscopy and computed tomography. *Nat Photon* 2009;**3**:503
69. Larina IV, Larin KV, Esenaliev RO. Real-time optoacoustic monitoring of temperature in tissues. *J Phys D* 2005;**38**:2633–9
70. Petrova EV, Brecht HP, Motamedi M, Oraevsky AA, Ermilov SA. In vivo optoacoustic temperature imaging for image-guided cryotherapy of prostate cancer. *Phys Med Biol* 2018;**63**:064002
71. Zhang HF, Maslov K, Stoica G, Wang LV. Functional photoacoustic microscopy for high-resolution and noninvasive in vivo imaging. *Nat Biotechnol* 2006;**24**:848–51
72. Yao J, Maslov KI, Shi Y, Taber LA, Wang LV. In vivo photoacoustic imaging of transverse blood flow by using doppler broadening of bandwidth. *Opt Lett* 2010;**35**:1419–21
73. Moore C, Jokerst JV. Strategies for Image-Guided therapy, surgery, and drug delivery using photoacoustic imaging. *Theranostics* 2019;**9**:1550–71
74. Iskander-Rizk S, van der Steen AFW, van Soest G. Photoacoustic imaging for guidance of interventions in cardiovascular medicine. *Phys Med Biol* 2019;**64**:16TR01
75. Karlas A, Fasoula N-A, Paul-Yuan K, Reber J, Kallmayer M, Bozhko D, Seeger M, Eckstein H-H, Wildgruber M, Ntziachristos V.

Cardiovascular optoacoustics: from mice to men – a review. *Photoacoustics* 2019;**14**:19–30
76. Mari JM, Xia W, West SJ, Desjardins AE. Interventional multispectral photoacoustic imaging with a clinical ultrasound probe for discriminating nerves and tendons: an ex vivo pilot study. *J Biomed Opt* 2015;**20**:110503
77. Xia W, Maneas E, Nikitichev DI, Mosse CA, Sato Dos Santos G, Vercauteren T, David AL, Deprest J, Ourselin S, Beard PC, Desjardins AE. Interventional photoacoustic imaging of the human placenta with ultrasonic tracking for minimally invasive fetal surgeries. *Med Image Comput Comput Assist Interv* 2015;**9349**:371–8
78. Kim C, Erpelding TN, Akers WJ, Maslov K, Song L, Jankovic L, Margenthaler JA, Achilefu S, Wang LV. Photoacoustic image-guided needle biopsy of sentinel lymph nodes. *SPIE* 2011;**7899**:78990K
79. Xi L, Zhou G, Gao N, Yang L, Gonzalo DA, Hughes SJ, Jiang H. Photoacoustic and fluorescence image-guided surgery using a multifunctional targeted nanoprobe. *Ann Surg Oncol* 2014;**21**:1602–9
80. Yaseen MA, Ermilov SA, Brecht HP, Su R, Conjusteau A, Fronheiser M, Bell BA, Motamedi M, Oraevsky AA. Optoacoustic imaging of the prostate: development toward image-guided biopsy. *J Biomed Opt* 2010;**15**:021310
81. Du L, Qin H, Ma T, Zhang T, Xing D. In vivo imaging-guided photothermal/photoacoustic synergistic therapy with bioorthogonal metabolic Glycoengineering-Activated tumor targeting nanoparticles. *ACS Nano* 2017;**11**:8930–43
82. Cui H, Yang X. In vivo imaging and treatment of solid tumor using integrated photoacoustic imaging and high intensity focused ultrasound system. *Med Phys* 2010;**37**:4777–81
83. Shangguan H, Casperson LW, Shearin A, M.D KWG, Prahl SA. Photoacoustic drug delivery: the effect of laser parameters on the spatial distribution of delivered drug. *SPIE* 1995;**2391**:394–402
84. Shangguan H, Casperson LW, Shearin A, Prahl SA. Investigation of cavitation bubble dynamics using particle image velocimetry: implications for photoacoustic drug delivery. *SPIE* 1996;**2671**:104–15
85. Di J, Kim J, Hu Q, Jiang X, Gu Z. Spatiotemporal drug delivery using laser-generated-focused ultrasound system. *J Control Rel* 2015;**220**:592–9
86. Xia J, Kim C, Lovell JF. Opportunities for photoacoustic-guided drug delivery. *Curr Drug Targets* 2015;**16**:571–81
87. Zhang Y, Yu J, Kahkoska AR, Gu Z. Photoacoustic drug delivery. *Sensors* 2017;**17**:1400
88. Furdella KJ, Witte RS, Geest JPV. Tracking delivery of a drug surrogate in the porcine heart using photoacoustic imaging and spectroscopy. *J Biomed Opt* 2017;**22**:041016
89. Moon GD, Choi S-W, Cai X, Li W, Cho EC, Jeong U, Wang LV, Xia Y. A new theranostic system based on gold nanocages and phase-change materials with unique features for photoacoustic imaging and controlled release. *J Am Chem Soc* 2011;**133**:4762–5
90. Duan Z, Gao Y-J, Qiao Z-Y, Fan G, Liu Y, Zhang D, Wang H. A photoacoustic approach for monitoring the drug release of pH-sensitive poly(*β*-amino ester)s. *J Mater Chem B* 2014;**2**:6271–82
91. Zhong J, Yang S, Wen L, Xing D. Imaging-guided photoacoustic drug release and synergistic chemo-photoacoustic therapy with paclitaxel-containing nanoparticles. *J Control Rel* 2016;**226**:77–87
92. Rajian JR, Fabiilli ML, Fowlkes JB, Carson PL, Wang X. Drug delivery monitoring by photoacoustic tomography with an ICG encapsulated double emulsion. *Opt Exp* 2011;**19**:14335–47
93. Berndl ESL, Hysi E, Hernandez C, Exner AA, Kolios MC. Using ultrasound and photoacoustics to monitor in situ forming implant structure and drug release. In: *IEEE international ultrasonics symposium (IUS)*, Washington, DC, USA, 6-9 Sep 2017
94. Cash KJ, Li C, Xia J, Wang LV, Clark HA. Optical drug monitoring: photoacoustic imaging of nanosensors to monitor therapeutic lithium in vivo. *ACS Nano* 2015;**9**:1692–8
95. Yang Z, Song J, Tang W, Fan W, Dai Y, Shen Z, Lin L, Cheng S, Liu Y, Niu G, Rong P, Wang W, Chen X. Stimuli-Responsive nanotheranostics for Real-Time monitoring drug release by photoacoustic imaging. *Theranostics* 2019;**9**:526–36
96. Jeevarathinam AS, Pai N, Huang K, Hariri A, Wang J, Bai Y, Wang L, Hancock T, Keys S, Penny W, Jokerst JV. A cellulose-based photoacoustic sensor to measure heparin concentration and activity in human blood samples. *Biosens Bioelectron* 2019;**126**:831–7
97. Schäfer-Korting M. *Drug delivery.* **Vol. 197**. Berlin: Springer Science & Business Media, 2010
98. Ray PC, Khan SA, Singh AK, Senapati D, Fan Z. Nanomaterials for targeted detection and photothermal killing of bacteria. *Chem Soc Rev* 2012;**41**:3193–209
99. Jaque D, Martínez Maestro L, del Rosal B, Haro-Gonzalez P, Benayas A, Plaza JL, Martín Rodríguez E, García Solé J. Nanoparticles for photothermal therapies. *Nanoscale* 2014;**6**:9494–530
100. Jung HS, Verwilst P, Sharma A, Shin J, Sessler JL, Kim JS. Organic molecule-based photothermal agents: an expanding photothermal therapy universe. *Chem Soc Rev* 2018;**47**:2280–97
101. Manivasagan P, Quang Bui N, Bharathiraja S, Santha Moorthy M, Oh YO, Song K, Seo H, Yoon M, Oh J. Multifunctional biocompatible chitosan-polypyrrole nanocomposites as novel agents for photoacoustic imaging-guided photothermal ablation of cancer. *Sci Rep* 2017;**7**:43593
102. Guo B, Sheng Z, Hu D, Liu C, Zheng H, Liu B. Through scalp and skull NIR-II photothermal therapy of deep orthotopic brain tumors with precise photoacoustic imaging guidance. *Adv Mater* 2018;**30**:1802591
103. Fan B, Yang X, Li X, Lv S, Zhang H, Sun J, Li L, Wang L, Qu B, Peng X, Zhang R. Photoacoustic-imaging-guided therapy of functionalized melanin nanoparticles: combination of photothermal ablation and gene therapy against laryngeal squamous cell carcinoma. *Nanoscale* 2019;**11**:6285–96
104. Shah J, Park S, Aglyamov S, Larson T, Ma L, Sokolov K, Johnston K, Milner T, Emelianov SY. Photoacoustic imaging and temperature measurement for photothermal cancer therapy. *J Biomed Opt* 2008;**13**:034024
105. Kim S, Chen YS, Luke GP, Emelianov SY. In-vivo ultrasound and photoacoustic image- guided photothermal cancer therapy using silica-coated gold nanorods. *IEEE Trans Ultrason Ferroelect Freq Contr* 2014;**61**:891–7
106. Song J, Yang X, Jacobson O, Lin L, Huang P, Niu G, Ma Q, Chen X. Sequential drug release and enhanced photothermal and photoacoustic effect of hybrid reduced graphene oxide-loaded ultrasmall gold nanorod vesicles for cancer therapy. *ACS Nano* 2015;**9**:9199–209
107. Liang S, Li C, Zhang C, Chen Y, Xu L, Bao C, Wang X, Liu G, Zhang F, Cui D. CD44v6 monoclonal Antibody-Conjugated gold nanostars for targeted photoacoustic imaging and plasmonic photothermal therapy of gastric cancer stem-like cells. *Theranostics* 2015;**5**:970–84
108. Yu J, Yang C, Li J, Ding Y, Zhang L, Yousaf MZ, Lin J, Pang R, Wei L, Xu L, Sheng F, Li C, Li G, Zhao L, Hou Y. Multifunctional Fe5C2 nanoparticles: a targeted theranostic platform for magnetic resonance imaging and photoacoustic tomography-guided photothermal therapy. *Adv Mater* 2014;**26**:4114–20
109. Mou J, Li P, Liu C, Xu H, Song L, Wang J, Zhang K, Chen Y, Shi J, Chen H. Ultrasmall Cu2-x S nanodots for highly efficient photoacoustic Imaging-Guided photothermal therapy. *Small* 2015;**11**:2275–83
110. Zhang Y, Wang L, Liu L, Lin L, Liu F, Xie Z, Tian H, Chen X. Engineering metal–organic frameworks for photoacoustic Imaging-Guided chemo-/photothermal combinational tumor therapy. *ACS Appl Mater Interfaces* 2018;**10**:41035–45
111. Jin Y, Li Y, Ma X, Zha Z, Shi L, Tian J, Dai Z. Encapsulating tantalum oxide into polypyrrole nanoparticles for X-ray CT/photoacoustic bimodal imaging-guided photothermal ablation of cancer. *Biomaterials* 2014;**35**:5795–804
112. Li Y, Jiang C, Zhang D, Wang Y, Ren X, Ai K, Chen X, Lu L. Targeted polydopamine nanoparticles enable photoacoustic imaging guided chemo-photothermal synergistic therapy of tumor. *Acta Biomater* 2017;**47**:124–34
113. Santha Moorthy M, Hoang G, Subramanian B, Bui NQ, Panchanathan M, Mondal S, Thi Tuong VP, Kim H, Oh J. Prussian blue decorated mesoporous silica hybrid nanocarriers for photoacoustic imaging-guided synergistic chemo-photothermal combination therapy. *J Mater Chem B* 2018;**6**:5220–33

114. Rai P, Mallidi S, Zheng X, Rahmanzadeh R, Mir Y, Elrington S, Khurshid A, Hasan T. Development and applications of photo-triggered theranostic agents. *Adv Drug Deliv Rev* 2010;**62**:1094–124
115. Fomina N, Sankaranarayanan J, Almutairi A. Photochemical mechanisms of light-triggered release from nanocarriers. *Adv Drug Deliv Rev* 2012;**64**:1005–20
116. Shubert J, Lediju Bell MA. Photoacoustic imaging of a human vertebra: implications for guiding spinal fusion surgeries. *Phys Med Biol* 2018;**63**:144001
117. Matthews TP, Zhang C, Yao DK, Maslov K, Wang LV. Label-free photoacoustic microscopy of peripheral nerves. *J Biomed Opt* 2014;**19**:16004
118. Yang J-M, Favazza C, Chen R, Yao J, Cai X, Maslov K, Zhou Q, Shung KK, Wang LV. Simultaneous functional photoacoustic and ultrasonic endoscopy of internal organs in vivo. *Nat Med* 2012;**18**:1297
119. Horiguchi A, Tsujita K, Irisawa K, Kasamatsu T, Hirota K, Kawaguchi M, Shinchi M, Ito K, Asano T, Shinmoto H, Tsuda H, Ishihara M. A pilot study of photoacoustic imaging system for improved real-time visualization of neurovascular bundle during radical prostatectomy. *Prostate* 2016;**76**:307–15
120. Thawani JP, Amirshaghaghi A, Yan L, Stein JM, Liu J, Tsourkas A. Photoacoustic-Guided surgery with indocyanine Green-Coated superparamagnetic iron oxide nanoparticle clusters. *Small* 2017;**13**:1701300
121. Lee HJ, Liu Y, Zhao J, Zhou M, Bouchard RR, Mitcham T, Wallace M, Stafford RJ, Li C, Gupta S, Melancon MP. In vitro and in vivo mapping of drug release after laser ablation thermal therapy with doxorubicin-loaded hollow gold nanoshells using fluorescence and photoacoustic imaging. *J Control Rel* 2013;**172**:152–8
122. Kim T, Zhang Q, Li J, Zhang L, Jokerst J. A gold/silver hybrid nanoparticle for treatment and photoacoustic imaging of bacterial infection. *ACS Nano* 2018;**12**:
123. Lemaster JE, Chen F, Kim T, Hariri A, Jokerst JV. Development of a trimodal contrast agent for acoustic and magnetic particle imaging of stem cells. *ACS Appl Nano Mater* 2018;**1**:1321–31
124. Dhada KS, Hernandez DS, Suggs LJ. In vivo photoacoustic tracking of mesenchymal stem cell viability. *ACS Nano* 2019;**13**:7791–9
125. Shubert J, Bell MAL. Photoacoustic based visual servoing of needle tips to improve biopsy on obese patients. In: *IEEE international ultrasonics symposium (IUS)*, Washtington, DC, USA, 6-9 Sep 2017
126. Hariri A, Zhao E, Jeevarathinam AS, Lemaster J, Zhang J, Jokerst JV. Molecular imaging of oxidative stress using an LED-based photoacoustic imaging system. *Sci Rep* 2019;**9**:11378
127. Chen Q, Xie H, Xi L. Wearable optical resolution photoacoustic microscopy. *J Biophotonics* 2019;**12**:e201900066
128. Moore C, Bai Y, Hariri A, Sanchez JB, Lin C-Y, Koka S, Sedghizadeh P, Chen C, Jokerst JV. Photoacoustic imaging for monitoring periodontal health: a first human study. *Photoacoustics* 2018;**12**:67–74